



Design and Characterization of Phosphate-Containing Ceramics with Kosnarite- and Langbeinite-Type Structures for Industrial Applications

Vladimir I. Pet'kov*, Elena A. Asabina, Maksim V. Sukhanov, Igor A. Schelokov, Aleksander S. Shipilov, Artem A. Alekseev

Lobachevsky State University of Nizhni Novgorod, Pr. Gagarina 23, Nizhni Novgorod, 603950 Russian Federation
petkov@inbox.ru

Crystal-chemical approach provided the scientific basis for the design of new compounds with desirable structure and properties. We systemized our and literature data on the synthesis, structures and physicochemical characteristics of complex anhydrous phosphates formed by cations in oxidation degrees ranging from +1 to +4 (M^+ – Li, Na, K, Rb, Cs; M^{2+} – Mg, Ca, Sr, Ba, Mn, Co, Ni, Cu, Zn; M^{3+} – Fe, M^{4+} – Ti, Zr, Hf), including phosphates in which PO_4 has been partially replaced by TO_4 ($T = Si, As, V, Mo, S$). To study the influence of M^+ and M^{4+} , M^{2+} and M^{4+} radii on the stability regions of different structural types, we studied the phase formation in the $M^{+1-x}M^{+x}M^{4+}_2(PO_4)_3$, $M^+Zr_2(TO_4)_x(PO_4)_{3-x}$, $M^{2+}_{0.5+x}M^{2+}_xM^{4+}_{2-x}(PO_4)_3$, $Ba_{3/2}Fe_2(PO_4)_3$, $M^+M^{2+}MgM^{4+}(PO_4)_3$, $M^{+5/3}MgM^{4+}_{4/3}(PO_4)_3$ and $M^{2+}_{0.5(1+x)}Fe_xTi_{2-x}(PO_4)_3$ systems with smoothly varying compositions. The key factors responsible for the formation of a particular type of structure are analyzed. The possibilities are considered for preparing structures of a desired type and for fine tuning of properties of obtained ceramics by varying the cationic and anionic components of the phosphate with retention of stable structural fragments of the crystal ensemble.

1. Introduction

Progress in the solid state chemistry is largely associated with creating multicomponent chemical substances, developing new processes (including synthesis) and conditions of materials processing. Complex anhydrous phosphates formed by cations in oxidation degrees ranging from +1 to +4 are of interest as hi-tech ceramic basis due to their high stability against high temperature, aggressive media and radiation, as well as their near-zero thermal expansion, high ionic conductivity and catalytic activity (Pet'kov, 2012). The multifunctional character of such ceramics allows them to be used in the fabrication of engineering materials, including parts of engines, lining tiles, precision-soldering accessories, semiconductor substrates, catalyst supports, radiation-resistant toxic waste forms, as well as solid electrolytes for batteries and sensors, fuel cells, selective catalysts, and luminescent materials.

The structural frameworks of the considered phosphates are formed by $L_2(PO_4)_3$ fragments from corner-shared two LO_6 -octahedra and three PO_4 -tetrahedra. Different linking variants of $L_2(PO_4)_3$ fragments lead to several structural types of the phosphates (Figure 1). The structural types of $NaZr_2(PO_4)_3$ (NZN/NASICON, mineral analog is kosnarite $KZr_2(PO_4)_3$, sp. gr. $R\bar{3}c$), $Sc_2(WO_4)_3$ (SW, sp. gr. $P2_1/n$) and $K_2Mg_2(SO_4)_3$ (KMS, langbeinite, sp. gr. $P2_13$) are well-known (Pet'kov, 2012).

The NZP structure has two types of framework cavity sites: six-fold M1 and eight-fold M2. Structure-forming L cations with mainly covalent metal–oxygen bonds usually have medium ionic radii (about 0.6...0.8 Å) and high oxidation degrees (+5...+3), and M sites are preferably occupied by cations with larger sizes and oxidation degrees +1 and +2.

The SW structure has several (depending on structure deformation) M-sites, surrounded by four-five nearest O atoms, in the framework cavities. The sizes of the cavity cations are usually smaller than those in the case of NZP structure and just slightly larger than the framework cation sizes.

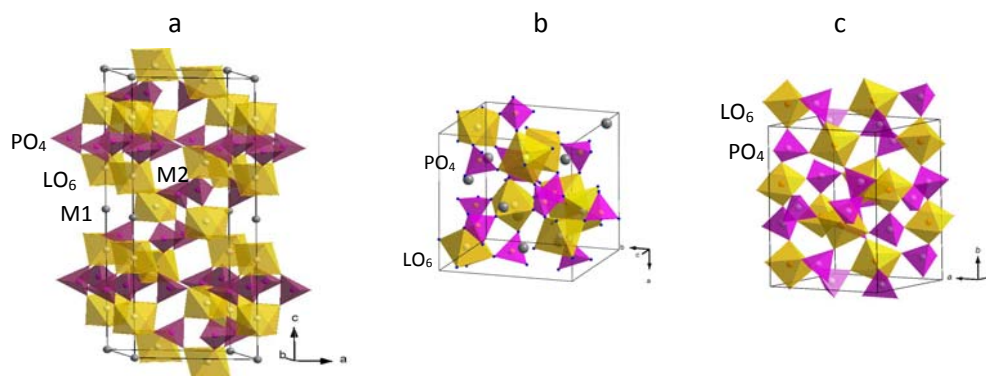


Figure 1: $L_2(PO_4)_3$ fragments in different structural types: (a) NZP (M1 and M2 – cavity sites); (b) SW; (c) langbeinite.

The langbeinite structure contains two types of M interstitial positions surrounded by six-twelve (usually nine) O atoms. So this structure is typical of the phosphates containing large cations (more than 1.5 Å ionic radii) with low oxidation degrees (+1 and +2) in the cavity sites.

The aim of the present work is to describe the synthesis, the phase formation in the $M^{1-x}M^{1+}_xM^{4+}_2(PO_4)_3$, $M^+Zr_2(TO_4)_x(PO_4)_{3-x}$, $M^{2+0.5+x}M^{2+}_xM^{4+}_{2-x}(PO_4)_3$, $Ba_{3/2}Fe_2(PO_4)_3$, $M^+M^{2+}MgM^{4+}(PO_4)_3$, $M^{5/3}MgM^{4+}_{4/3}(PO_4)_3$ and $M^{2+0.5(1+x)}Fe_xTi_{2-x}(PO_4)_3$ systems with smoothly varying compositions (M^+ – Li, Na, K, Rb, Cs; M^{2+} – Mg, Ca, Sr, Ba, Mn, Co, Ni, Cu, Zn; M^{3+} – Fe, M^{4+} – Ti, Zr, Hf), including phosphates in which PO_4 has been partially replaced by TO_4 (T = Si, As, V, Mo, S), to examine in detail the influence of M^+ and M^{4+} , M^{2+} and M^{4+} cationic radii on the stability regions of different structural types, and to demonstrate the ways of practical application of the ceramics taking into account their structural features.

2. Experimental

The complex phosphates $M^{1-x}M^{1+}_xM^{4+}_2(PO_4)_3$ (M^+ , M^{1+} – Li, Na, K, Rb, Cs) and $M^{2+0.5+x}M^{2+}_xM^{4+}_{2-x}(PO_4)_3$ (M^{2+} , M^{2+} – Ca, Sr, Ba, Mn, Co, Ni, Cu, Zn) with pairs of different metals M^+ and M^+ (or M^{2+} and M^{2+}), $Ba_{3/2}Fe_2(PO_4)_3$, $M^+M^{2+}MgM^{4+}(PO_4)_3$, $M^{5/3}MgM^{4+}_{4/3}(PO_4)_3$, $M^{2+0.5(1+x)}Fe_xTi_{2-x}(PO_4)_3$ and the mixed phosphates $M^+Zr_2(TO_4)_x(PO_4)_{3-x}$ (T – As, V) and $M^{1-x}Zr_2(TO_4)_x(PO_4)_{3-x}$ (T – S, Mo) were synthesized by sol-gel method (M^{4+} – Ti, Zr) and solid-state reactions (M^{4+} – Hf). The starting materials for their synthesis were the salts (chlorides, nitrates, carbonates) of metals M^+ and M^{2+} , $FeCl_3$, $TiOCl_2$, $ZrOCl_2$, HfO_2 , H_3PO_4 or $NH_4H_2PO_4$, H_3AsO_4 , NH_4VO_3 , H_2SO_4 and $(NH_4)_6Mo_7O_{24} \cdot 4H_2O$ of chemically pure grade.

In accordance to the sol-gel method the aqueous solutions of the starting reactants were mixed under continuous stirring. Afterwards, the reaction mixture was dried at 90 °C and thermally processed in unconfirmed air access at 600, 800 and 900 °C for at least 24 h at each stage. According to solid-state method, a fine mixture of the stoichiometric amounts of the reactants was dried at 200 °C for 10 – 16 h, and then thermally processed in unconfirmed air access at 600 °C K and 800 – 1 200 °C with a step interval of 100 °C for at least 24 h at each stage. The obtained samples were polycrystalline powders. Their chemical composition and homogeneity were checked with the aid of a CamScan MV-2300 microprobe with a Link INCA ENERGY 200C energy-dispersion detector. The uncertainty of the chemical composition determination was within 2 % mass.

Phase purity was established by powder X-ray diffraction (XRD) at Shimadzu XRD-6000 diffractometer ($CuK\alpha$ radiation). High temperature studies were carried out in the range from room temperature to 800°C on the same diffractometer equipped with a Shimadzu HA-1001 sample heating attachment. Unit cell parameters were determined from the corresponding diffraction patterns indexed within 2θ range 10 – 60°. The data for the structure refinement were collected between 2θ 5 – 110° with a step interval of 0.02°. Structure refinements were performed by the Rietveld method with Rietan-97 program.

The functional composition of the samples was confirmed by IR spectroscopy on a Shimadzu FTIR 8400S spectrometer within the range of 1 400 – 400 cm^{-1} .

3. Phase formation of complex and mixed phosphates

The main approaches to the synthesis of powders and single crystals of the phosphates are based on the reactions taking place in: (a) solid phases, (b) aqueous or organic solutions (sol-gel and hydrothermal methods), (c) in melts. The solid state method of $M^{1-x}M^{1+}_xHf_2(PO_4)_3$ (M^+ , M^{1+} – Li, Na, K, Rb, Cs) synthesis allows us to obtain high-purity substances for structural and other investigations. Unfortunately this method

requires a long time of thermal treatment stages, using high temperatures of synthesis and the careful grinding of reaction mixture. Synthesis by sol-gel method may be performed in aqueous solutions or organic media (Pechini method). Its advantages are synthesis procedure simplicity, high composition control and powder particle size, a short time and low temperature of thermal treatment. Synthesis in melt allows us to obtain $\text{Ba}_{1.5}\text{Fe}_2(\text{PO}_4)_3$ single crystals, but it requires using of high temperatures.

The compounds described by the formula $\text{M}^+\text{M}^{4+}_2(\text{PO}_4)_3$ are most widely distributed among double phosphates of M^+ and M^{4+} cations (Table 1). Many representatives of the phosphates belong to NZP structure with trigonal symmetry. The occupation of M1 sites by large ions leads an increase in parameter c and corresponding deformation of PO_4 tetrahedra lead to parameter a reducing (Figure 1). The compounds are characterized by high thermal stability. The melting (decomposition) temperatures of $\text{M}^+\text{Zr}_2(\text{PO}_4)_3$ with $\text{M}^+ - \text{Li}, \text{Na}, \text{K}$ are 1690, 1650 and 1610 °C, correspondingly.

So, in spite of structural distortions in NZP type compounds, the basic structural motive stays invariable. The main structural feature of NZP-, SW- or KMS-type phosphates is belonging to the types with $\{[\text{L}_2(\text{PO}_4)_3]^{3-}\}_3$ frameworks. This fact allows wide variation possibilities for cations in all structural sites. Based on the crystal chemical approach, we predicted, synthesized and investigated the phases of variable compositions $\text{M}^{1-x}\text{M}^{4+x}\text{M}^{4+}_2(\text{PO}_4)_3$ ($\text{M}^+, \text{M}^+ - \text{Li}, \text{Na}, \text{K}, \text{Rb}, \text{Cs}$) of NZP type structure. The crystallographic parameters of solid solutions smoothly change within the regions of solid solution formation (Figure 2a). IR spectra gradually change with the smooth change of phosphates compositions (Figure 2b). Structural investigation by the Rietveld method revealed that alkali metal cations in the $\text{Na}_{0.5}\text{K}_{0.5}\text{M}^{4+}_2(\text{PO}_4)_3$ ($\text{M}^{4+} - \text{Ti}, \text{Hf}$), $\text{K}_{0.5}\text{Rb}_{0.5}\text{Ti}_2(\text{PO}_4)_3$ and $\text{Li}_{0.5}\text{K}_{0.5}\text{Hf}_2(\text{PO}_4)_3$ were statistically distributed in completely occupied M1 sites.

Table 1: Literature data on the structures of $\text{M}^+\text{M}^{4+}_2(\text{PO}_4)_3$ compounds (Pet'kov, 2012)

Substance	Space group (crystal system)	Substance	Space group (crystal system)	Substance	Space group (crystal system)
$\text{M}^+\text{Ti}_2(\text{PO}_4)_3$ ($\text{M}^+ - \text{Li}, \text{Na}, \text{K}, \text{Rb}, \text{NH}_4, \text{Cu}$)	$R\bar{3}c$	$\text{M}^+\text{Hf}_2(\text{PO}_4)_3$ ($\text{M}^+ - \text{Na}, \text{K}, \text{Rb}, \text{Cs}, \text{Cu}, \text{Ag}$)	$R\bar{3}c$	$\text{M}^+\text{Sn}_2(\text{PO}_4)_3$ ($\text{M}^+ - \text{Cu}, \text{Ag}$)	$R\bar{3}c$
$\text{CsTi}_2(\text{PO}_4)_3$	$1a\bar{3}d$	$\text{LiGe}_2(\text{PO}_4)_3$	$R\bar{3}c$	$\text{NaTh}_2(\text{PO}_4)_3$	Cc
$\text{LiZr}_2(\text{PO}_4)_3$	$R\bar{3}c, C\bar{1}, P2_1/n, Pbn$	$\text{M}^+\text{Ge}_2(\text{PO}_4)_3$ ($\text{M}^+ - \text{Na}, \text{K}$)	$R\bar{3}$	$\text{M}^+\text{Th}_2(\text{PO}_4)_3$ ($\text{M}^+ - \text{K}, \text{NH}_4$)	$C2/c$
$\text{M}^+\text{Zr}_2(\text{PO}_4)_3$ ($\text{M}^+ - \text{Na}, \text{K}, \text{Rb}, \text{Cs}, \text{H}, \text{NH}_4, \text{Cu}$)	$R\bar{3}c$	$\text{NaGeTi}(\text{PO}_4)_3$	$R\bar{3}$	$\text{KU}_2(\text{PO}_4)_3$	$R\bar{3}c, C2/c$
$\text{LiHf}_2(\text{PO}_4)_3$	$R\bar{3}c, P\bar{1}$	$\text{LiSn}_2(\text{PO}_4)_3$	$R\bar{3}c, P\bar{1}$	$\text{RbU}_2(\text{PO}_4)_3$	$R\bar{3}c$
		$\text{NaSn}_2(\text{PO}_4)_3$	$R\bar{3}c, R\bar{3}$	$\text{NaPu}_2(\text{PO}_4)_3$	Trigonal, Cc
				$\text{KPu}_2(\text{PO}_4)_3$	$R\bar{3}c$, Monoclinic
				$\text{RbPu}_2(\text{PO}_4)_3$	Trigonal

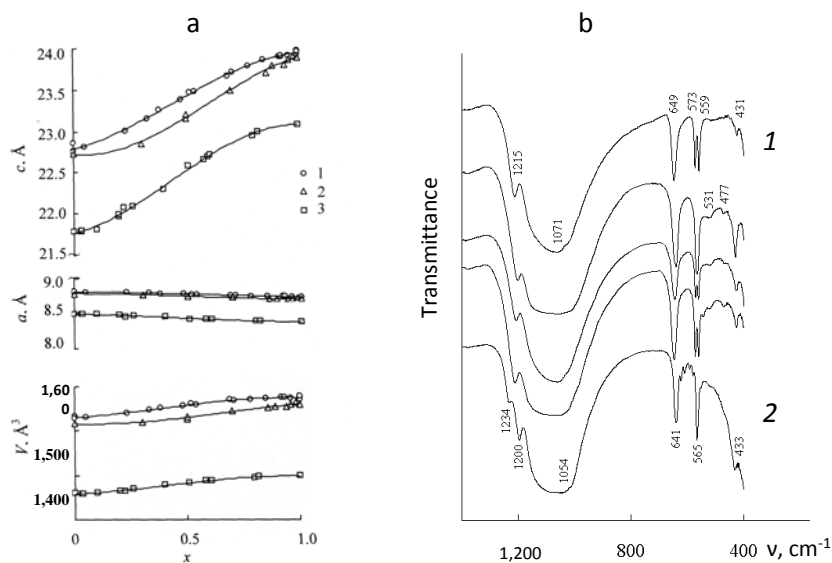


Figure 2: (a) Unit cell parameters of $\text{Na}_{1-x}\text{K}_x\text{M}^{4+}_2(\text{PO}_4)_3$ vs. composition: (1) $\text{M}^{4+} - \text{Zr}$, (2) $\text{M}^{4+} - \text{Hf}$, (3) $\text{M}^{4+} - \text{Ti}$. (b) IR spectra of $\text{K}_{1-x}\text{Cs}_x\text{Hf}_2(\text{PO}_4)_3$: (1) $x = 0$; (2) $x = 0.3$; (3) $x = 0.5$; (4) $x = 0.7$; (5) $x = 1.0$.

Concentration limits of solid solution existence in the systems of Ti-, Zr- and Hf-phosphates depend on the relative difference in bond lengths of alkali metal–oxygen $\Delta d/d_1$ in double phosphates $M^+M^{4+}_2(PO_4)_3$ and $M^{+}M^{4+}_2(PO_4)_3$ (Table 2). Continuous solid solutions may exist at room temperature if $\Delta d/d_1$ does not exceed 11% (except $Li_{1-x}K_xHf_2(PO_4)_3$ system). There are no noticeable solid solutions in the systems with $\Delta d/d_1 \geq 21\%$. As ionic radii of Hf^{4+} (0.71 Å) and Zr^{4+} (0.72 Å) are almost identical, there are almost the same phase formation regularities in the systems of zirconium and hafnium containing phosphates. The forming of continuous solid solutions in the $Li_{1-x}K_xHf_2(PO_4)_3$ system is caused by the effect of the hafnium electronic structure, leading to the stability of $LiHf_2(PO_4)_3$ rhombohedral modification (compared with $LiZr_2(PO_4)_3$). Lower concentration limits of NZP structure in titanium phosphates may be explained by the small ionic radius of the framework forming cation Ti^{4+} (0.61 Å) and the difficulty of the incorporation of large cations Cs^+ in the cavities of NZP $[Ti_2(PO_4)_3]^-$ framework. $CsTi_2(PO_4)_3$ phosphate crystallizes in the structure with another spatial connection of framework-forming polyhedra. So, the cavity cation radius has influence on the stability of the given framework type.

Table 2: Concentration regions of NZP solid solutions in the $M^{+}_{1-x}M^{4+}_xM^{4+}_2(PO_4)_3$ ($M^{4+} - Ti, Zr, Hf$) systems

M	M'	Ti		Zr		Hf
		x	$\Delta d/d_1^a, \%$	X	$\Delta d/d_1^a, \%$	x
Li	Na	0 – 1	9	0 – 1	11	0 – 1
	K	Phase mixture	21	Phase mixture	24	0 – 1
Na	K	0 – 1	11	0 – 1	10	0 – 1
	Rb	0 – 0.3, 0.7 – 1	15	0 – 1	11	0 – 1
	Cs	0 – 0.2	–	0 – 0.3, 0.7 – 1	13	0 – 0.3, 0.7 – 1
K	Rb	0 – 1	4	0 – 1	1	0 – 1
	Cs	0 – 0.3	–	0 – 1	3	0 – 1
Rb	Cs	Phase mixture	–	0 – 1	2	0 – 1

$$^a d/d_1 = (d_{M-O} - d_{M-O})/d_{M-O}.$$

The XRD and IR spectroscopy results showed that phosphates of the compositions $M_{0.5+x}M'_xZr_{2-x}(PO_4)_3$ ($M - Co, Mn$; $M' - Mg, Co, Mn$) crystallized in the SW and NZP structural types (Table 3). Optimal conditions for SW structure formation exist in the case when the average ionic radius of cavities cations is a little bit higher compared with those of framework-forming cations. If their size difference is more significant (like in Ca-containing samples), NZP structure is formed in high concentration range x.

The influence of framework-forming M^{2+} cation nature on its isomorphic substitution of Zr^{4+} is clearly observed in the SW systems. The widest solid solutions regions were formed in the Mg-containing phosphates rows, that may be explained by the closeness of Mg^{2+} and Zr^{4+} ionic radii ($r_{Mg^{2+}} = r_{Zr^{4+}} = 0.72$ Å) and electronegativities. The crystal structures of triple phosphates $MnMg_{0.5}Zr_{1.5}(PO_4)_3$, $CoMn_{0.5}Zr_{1.5}(PO_4)_3$ and $CaCo_{0.5}Zr_{1.5}(PO_4)_3$ ($x = 0.5$) were refined by the Rietveld method. The Co^{2+} , Mn^{2+} and Mg^{2+} cations (together with Zr^{4+}) form the structural framework. In SW phosphates $MnMg_{0.5}Zr_{1.5}(PO_4)_3$ and $CoMn_{0.5}Zr_{1.5}(PO_4)_3$, Mn^{2+} ($r = 0.66$ Å) and Co^{2+} ($r = 0.58$ Å) are situated in relatively small cavities of the SW structures, while Ca^{2+} ($r = 1.00$ Å) occupy comparatively large cavities of the NZP structure.

Table 3: Concentration regions of SW and NZP-type solid solutions in the $M_{0.5+x}M'_xZr_{2-x}(PO_4)_3$ ($M - Co, Mn, Ca, Ba$; $M' - Mg, Co, Mn$) systems

System	Concentration regions	Structural type
$Co_{0.5+x}[Mg_xZr_{2-x}(PO_4)_3]$	$0 \leq x \leq 1.0$	SW
	$1.0 < x \leq 2.0$	SW+(Co,Mg) ₃ (PO ₄) ₂
$Co_{0.5+x}[Co_xZr_{2-x}(PO_4)_3]$	$x = 0$	SW
	$0 < x \leq 2.0$	SW+Co ₃ (PO ₄) ₂
$Co_{0.5}Mn_x[Co_xZr_{2-x}(PO_4)_3]$	$0 \leq x \leq 0.5$	SW
	$0.5 < x \leq 2.0$	SW+(Co,Mn) ₃ (PO ₄) ₂
$Mn_{0.5+x}[Mg_xZr_{2-x}(PO_4)_3]$	$0 \leq x \leq 1.0$	SW
	$1.0 < x \leq 2.0$	SW+(Mn,Mg) ₃ (PO ₄) ₂
$Mn_{0.5+x}[Co_xZr_{2-x}(PO_4)_3]$	$x = 0$	SW
	$0 < x \leq 2.0$	SW+(Co,Mn) ₃ (PO ₄) ₂
$Mn_{0.5+x}[Mn_xZr_{2-x}(PO_4)_3]$	$0 \leq x \leq 0.5$	SW
	$0.5 < x \leq 2.0$	SW+Mn ₃ (PO ₄) ₂
$Ca_{0.5+x}[M'_xZr_{2-x}(PO_4)_3]$	$0 \leq x \leq 1.0$	NZP
	$1.0 < x \leq 2.0$	NZP+(Ca,M') ₃ (PO ₄) ₂

Some NZP phosphates contain PO_4 anions together with other tetrahedral anions. The solid solutions $\text{Na}_{1+x}\text{Zr}_2(\text{SiO}_4)_x(\text{PO}_4)_{3-x}$ ($0 \leq x \leq 3$) possess high cationic conductivity, that is why they are best studied (Anantharamulu, 2011). Depending on the composition of the silicophosphate, the symmetry varies from trigonal to monoclinic. Two continuous series of solid solutions, with NZP ($M = \text{Li}, \text{Na}, \text{K}, \text{Rb}, \text{Cs}$) and SW structure ($M = \text{Li}$), are formed in the $\text{MZr}_2(\text{AsO}_4)_x(\text{PO}_4)_{3-x}$ ($0 \leq x \leq 3$) systems (Pet'kov et al., 2014). The Li^+ ion can be tetrahedrally or octahedrally coordinated by oxygen, and this leads to the formation of the monoclinic or rhombohedral polymorphic modifications of $\text{LiZr}_2(\text{AsO}_4)_x(\text{PO}_4)_{3-x}$. The type of modification depends on the synthesis method, temperature and on the heat treatment time. Two zirconium phosphato-sulfates, α - and β - $\text{Zr}_2(\text{PO}_4)_2\text{SO}_4$, belong to the NZP and SW structural families accordingly. The β phase is the monoclinic distorted version of the α phase (Piffard et al, 1987).

Limited solid solutions $\text{M}_{1-x}\text{Zr}_2(\text{MoO}_4)_x(\text{PO}_4)_{3-x}$, where A is Na ($0 \leq x \leq 0.6$), K ($0 \leq x \leq 0.3$), Rb ($0 \leq x \leq 0.2$), or Cs ($0 \leq x \leq 0.1$) are formed in the systems studied (Pet'kov, 2012). The limited extents of the solid solutions are possible because of the alkali cation size and a significant difference between the molybdenum–oxygen bond lengths (1.65–1.77 Å) and phosphorus–oxygen bond lengths (1.50–1.55 Å). In the systems $\text{MZr}_2(\text{VO}_4)_x(\text{PO}_4)_{3-x}$, the NZP solid solutions are formed at the compositions $0 \leq x \leq 0.2$ for $M = \text{Li}$; $0 \leq x \leq 0.4$ for $M = \text{Na}$; $0 \leq x \leq 0.5$ for $M = \text{K}$; $0 \leq x \leq 0.3$ for $M = \text{Rb}$; and $0 \leq x \leq 0.2$ for $M = \text{Cs}$ (Pet'kov et al., 2013). Apart from the high temperature NZP-modification, $\text{LiZr}_2(\text{VO}_4)_x(\text{PO}_4)_{3-x}$ with $0 \leq x \leq 0.8$, synthesized at $T \leq 840^\circ\text{C}$ crystallizes in the SW structure. In spite of the acidic nature of V_2O_5 and P_2O_5 and relatively small difference between the V–O and P–O bond lengths in the VO_4 and PO_4 tetrahedra (~12%), considerable difference between the electronegativities ($\Delta = 0.56$) leads to the formation of the limited extents of the solid solutions.

$\text{Ba}_{3/2}\text{Fe}_2(\text{PO}_4)_3$, $\text{M}^+\text{M}^{2+}\text{MgM}^{4+}(\text{PO}_4)_3$ ($\text{M}^+ = \text{K}, \text{Rb}, \text{Cs}$, $\text{M}^{2+} = \text{Ba}, \text{Pb}$, $\text{M}^{4+} = \text{Ti}, \text{Zr}$), $\text{M}^{5/3}_2\text{MgM}^{4+}_{4/3}(\text{PO}_4)_3$ ($\text{M}^+ = \text{K}, \text{Rb}$, $\text{M}^{4+} = \text{Ti}, \text{Zr}$) systems belong to a wide family of compounds having KMS type structures (Pet'kov et al., 2010). The composition of the first compound was forecasted as the end member in the series of $\text{Ba}_{0.5(1+x)}\text{Fe}_x\text{M}_{2-x}(\text{PO}_4)_3$ ($M = \text{Ti}, \text{Zr}, \text{Hf}$) phosphates. According to Pet'kov et al. (2006), the $\text{M}^{2+}_{0.5(1+x)}\text{Fe}_x\text{M}^{4+}_{2-x}(\text{PO}_4)_3$ ($\text{M}^{2+} = \text{Mg}, \text{Ca}, \text{Sr}, \text{Ba}$; $\text{M}^{4+} = \text{Ti}, \text{Zr}, \text{Hf}$) series in the region $0 \leq x \leq 1.0$ form solid solutions of NZP structural type. The KMS structure is more favorable than the NZP for arrangement of a greater number of larger cations, such as Cs^+ and Ba^{2+} , in the cavities; however, the set of cations occupying different crystallographic positions and choice of the compound formulas is more limited.

4. Thermal expansion of phosphates with framework structures

Many complex phosphates may be used as high-technological ceramics with ultra-low thermal expansion, thermally stable and thermo-insulating materials and etc (Pet'kov, 2012). As the knowledge of thermophysical properties is necessary regardless of the field of substances practical using, we have studied thermal expansion behavior of the NZP phosphates.

Most of NZP compounds show thermal expansion anisotropy and large magnitudes of the linear thermal expansion coefficient (LTEC), but, nevertheless, low average TEC. When an NZP compound, for example, $\text{NaZr}_2(\text{PO}_4)_3$, is heated, the weakest Na–O bonds are elongated to a greater extent than the strong Zr–O and P–O bonds. On heating, the size of the trigonal antiprism around the Na site (M1 sites, see Figures 1a and 3) increases and elongates the column of polyhedra along the c axis ($\alpha_c > 0$); as a result, the ZrO_6 octahedra and PO_4 tetrahedra that share corners rotate, causing angular distortions in the polyhedra. The tetrahedral O–P–O angle increases along the c axis, the distance between the columns of the framework structure shortens, and the structure is compressed along the a axis ($\alpha_a < 0$). As a result, the average TEC of compounds is very low. Similarly, the best known low-expansion materials – zircon, cordierite and quartz glass – have almost zero average expansion [$\alpha_{av} = (0.5 \pm 4.2) \times 10^{-6} \text{ }^\circ\text{C}^{-1}$ in the temperature range of $0 \pm 1000 \text{ }^\circ\text{C}$].

Owing to the ultra-low thermal expansion (nearly-zero LTEC and expansion anisotropy), some phosphates of the NZP family can withstand repeated sharp changes of thermal load (thermal shocks) and are most promising for the fabrication of thermomechanically stable materials. The behaviour of NZP structure in response to heat treatment depends on the nature, the ratio of sizes and the number of cations that occupy crystallographic sites, the number of vacant sites and the unit cell symmetry. Pet'kov and Orlova (2003) proposed a system of empirical heat expansion rules for the lattice of NZP phosphates, which is suitable for extending the data to compounds that have not yet been studied and for targeted change in the thermal expansion characteristics. Thus, by combining the NZP compounds whose LTEC are similar in magnitude and have opposite signs and that form broad ranges of solid solutions, it is possible to predict ceramic compositions with controlled ultra-low thermal expansion.

The ways of practical application of phosphates as ionic conductors (with the controlling conductivity level) and selective catalysts, taking into account their structural features are described by Pet'kov (2012).

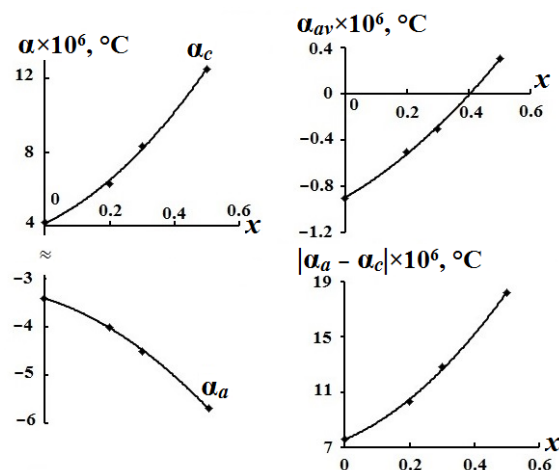


Figure 3: Dependences on vanadate-phosphates thermal expansion parameters vs. composition. Near-zero average thermal expansion coefficient is observed at $x = 0.4$.

5. Conclusions

The presented investigation reflects the extension of the range of objects and crystal structures of complex and mixed phosphates containing cations in oxidation degrees ranging from 1+ to 4+. The comparison of these compounds shows the similarity of formal features (composition, simple structural polyhedra) and allows us to identify some structural regularities depending on the size factor (cation ionic radii), the nature of cations and anions, and their electronegativities. The structures of complex and mixed phosphates of all presented types are composed of MO_6 , MO_9 , PO_4 polyhedra. The functions of the PO_4 tetrahedra can partly be performed by other tetrahedral TO_4 oxo anions.

Crystalline phosphates of the framework NZP, SW, KMS structure types are of interest because of their considerable thermal and chemical stability, resistance to radiation damage and other valuable physical and chemical properties that lead to industrial application possibilities as constructional and functional ceramics. The prospects of using mixed phosphates depend on the properties important for technical applications, which are either new or improved with respect to those of monoanionic phosphates.

Acknowledgements

The reported study was partially supported by RFBR, research project No. 15-03-00716 a.

References

- Anantharamulu N., Rao K.K., Rambabu G., Kumar B.V., Radha V., Vital M., 2011, A wide-ranging review on NASICON type materials, *J. Mater. Sci.* 46, 2821-2837.
- Pet'kov V.I., Orlova A.I., 2003, Crystal-chemical approach to predicting the thermal expansion of compounds in the NZP family, *Inorg. Mater.* 39, 1013–1024.
- Pet'kov V. I., Shchelokov I.A., Asabina E.A., Kurazhkovskaya V.S., Rusakov D.A., Pokholok K.V., Lazoryak B.I., 2006, Synthesis and phase formation in $\text{M}^{2+0.5(1+x)}\text{Fe}_x\text{Ti}_{2-x}(\text{PO}_4)_3$ phosphate series, *Russ. J. Inorg. Chem.* 51, 1855-1863.
- Pet'kov V. I., Shchelokov I.A., Surazhskaya M.D., Palkina K.K., Kanishcheva A.S., Knyazev A.V., 2010, Synthesis and crystal structure of phosphate $\text{Ba}_{1.5}\text{Fe}_2(\text{PO}_4)_3$, *Russ. J. Inorg. Chem.* 55, 1352-1355.
- Pet'kov V. I., 2012, Complex phosphates formed by metal cations in oxidation states I and IV, *Russ. Chem. Rev.* 81, 606-637.
- Pet'kov V. I., Sukhanov M.V., Shipilov A.S., Kurazhkovskaya V.S., Borovikova E.Yu., Sakharov N.V., Ermilova M.M., Orekhova N.V., 2013, Synthesis and structure of alkali metal zirconium vanadate phosphates, *Russ. J. Inorg. Chem.* 58, 1015-1021.
- Pet'kov V. I., Shipilov A.S., Sukhanov M.V., Kurazhkovskaya V.S., Borovikova E.Yu., 2014, Sol-gel synthesis and structure of $\text{MZr}_2(\text{AsO}_4)_3$ arsenates and $\text{MZr}_2(\text{AsO}_4)_x(\text{PO}_4)_{3-x}$ arsenate phosphates ($\text{M} = \text{K}, \text{Rb}, \text{Cs}$), *Russ. J. Inorg. Chem.* 59, 1201-1207.
- Piffard I., Verbaere A., Kinoshita M., 1987, $\beta\text{-Zr}_2(\text{PO}_4)_2\text{SO}_4$: A zirconium phosphato-sulfate with a $\text{Sc}_2(\text{WO}_4)_3$ structure. A comparison between Garnet, Nasicon, and $\text{Sc}_2(\text{WO}_4)_3$ structure types, *J. Solid State Chem.* 71, 121-130.